

## Measurement of Transverse Energy Production with Si and Au Beams at Relativistic Energy: Towards Hot and Dense Hadronic Matter

J. Barrette,<sup>(4)</sup> R. Bellwied,<sup>(10)</sup> S. Bennett,<sup>(10)</sup> P. Braun-Munzinger,<sup>(7)</sup> W. E. Cleland,<sup>(6)</sup> T. M. Cormier,<sup>(10)</sup> G. David,<sup>(7)</sup> J. Dee,<sup>(7)</sup> G. E. Diebold,<sup>(11)</sup> O. Dietzsch,<sup>(8)</sup> D. Fox,<sup>(3)</sup> J. V. Germani,<sup>(11)</sup> S. Gilbert,<sup>(4)</sup> S. V. Greene,<sup>(11)</sup> J. R. Hall,<sup>(5)</sup> T. K. Hemmick,<sup>(7)</sup> N. Herrmann,<sup>(2)</sup> B. Hong,<sup>(7)</sup> K. Jayananda,<sup>(6)</sup> D. Kraus,<sup>(6)</sup> B. Shiva Kumar,<sup>(11)</sup> R. Lacasse,<sup>(4)</sup> Q. Li,<sup>(10)</sup> D. Lissauer,<sup>(1)</sup> W. J. Llope,<sup>(7)</sup> T. W. Ludlam,<sup>(1)</sup> S. McCorkle,<sup>(1)</sup> R. Majka,<sup>(11)</sup> S. K. Mark,<sup>(4)</sup> R. Matheus,<sup>(10)</sup> J. T. Mitchell,<sup>(11)</sup> M. Muthuswamy,<sup>(7)</sup> E. O'Brien,<sup>(1)</sup> S. Panitkin,<sup>(7)</sup> C. Pruneau,<sup>(4)</sup> M. N. Rao,<sup>(7)</sup> M. Rosati,<sup>(4)</sup> F. Rotondo,<sup>(11)</sup> N. C. daSilva,<sup>(8)</sup> J. Simon-Gillo,<sup>(9)</sup> U. Sonnadara,<sup>(6)</sup> J. Stachel,<sup>(7)</sup> J. Sullivan,<sup>(3)</sup> H. Takai,<sup>(1)</sup> E. M. Takagui,<sup>(6)</sup> T. G. Throwe,<sup>(1)</sup> C. Winter,<sup>(11)</sup> G. Wang,<sup>(4)</sup> K. L. Wolf,<sup>(9)</sup> D. Wolfe,<sup>(5)</sup> C. L. Woody,<sup>(1)</sup> N. Xu,<sup>(7)</sup> Y. Zhang,<sup>(7)</sup> Z. Zhang,<sup>(6)</sup> and C. Zou<sup>(7)</sup>

(E814/E877 Collaboration)

<sup>(1)</sup> Brookhaven National Laboratory, Upton, New York 11973

<sup>(2)</sup> Gesellschaft für Schwerionenforschung, Darmstadt, Germany

<sup>(3)</sup> Los Alamos National Laboratory, Los Alamos, New Mexico 87545

<sup>(4)</sup> McGill University, Montreal, Canada

<sup>(5)</sup> University of New Mexico, Albuquerque, New Mexico 87131

<sup>(6)</sup> University of Pittsburgh, Pittsburgh, Pennsylvania 15260

<sup>(7)</sup> State University of New York, Stony Brook, New York 11794

<sup>(8)</sup> University of São Paulo, São Paulo, Brazil

<sup>(9)</sup> Texas A&M University, College Station, Texas 77843

<sup>(10)</sup> Wayne State University, Detroit, Michigan 48202

<sup>(11)</sup> Yale University, New Haven, Connecticut 06511

(Received 28 December 1992)

We present a systematic study of transverse energy ( $E_T$ ) production in collisions of 11.4A GeV/c Au and 14.6A GeV/c Si ions with targets of Al, Au, and Pb. Comparison of data for Au+Au and Si+Al indicates that, for the heavier system, there is an increase in the amount of stopping which is accompanied by a decrease in the width of the  $dE_T/d\eta$  distribution. The ratio of the maximum  $E_T$  observed for the two systems is significantly greater than the ratio of the total energy available in the center of mass frame.

PACS numbers: 25.75.+r

Global observables such as transverse energy  $E_T$  contain valuable information on the reaction dynamics and, albeit indirectly, on the energy and baryon density reached in relativistic nucleus-nucleus collisions. With light projectiles ( $A = 16-32$ )  $E_T$  production has been studied in detail previously both at AGS and CERN energies [1]. Large energy depositions have been inferred from these measurements. Extrapolating these results to heavy projectiles raises expectations to create, in these collisions, the predicted [2] deconfined phase of quarks and gluons. We report here measurements of the transverse energy distribution produced in collisions of 11.4A GeV/c  $^{197}\text{Au}$  beams with nuclear targets at the Brookhaven National Laboratory Alternating Gradient Synchrotron (AGS). Comparison to similar data obtained with Si beams at 14.6A GeV/c yields information, for the first time, on how the  $E_T$  distribution evolves with mass number from light to very heavy colliding systems. The new Au data provide evidence for the formation of hot and very dense matter.

Most aspects of the data obtained with light pro-

jectiles are explained qualitatively within a geometrical picture based on the number of nucleons in the overlap volume of target and projectile [1]. In this picture,  $E_T$  production is proportional to the available energy  $E^* = \sqrt{s} - m_N(N_p + N_t)$ . Here  $\sqrt{s}$  is the center of mass energy of the participating nucleons,  $m_N$  is the nucleon mass, and  $N_p$  and  $N_t$  are the number of participating projectile and target nucleons mapped out by the collision geometry. This approach provides a basis for comparison of  $E_T$  production for systems of different size and at different beam energies. For symmetric  $A + A$  collisions at impact parameter  $b = 0$ ,  $E^*$  reaches a maximum given by  $E^* = m_N A(\sqrt{2 + 2E_{\text{lab}}/Am_N} - 2)$ . For Si+Al and Au+Au at the present energies, the ratio of available energy for central collisions is  $E^*(\text{Au})/E^*(\text{Si}) = 5.9$ . The shape of differential cross sections  $d\sigma/dE_T$  reflects the geometric overlap modified by various fluctuations. Of particular interest to the present investigation is the search for deviations from this simple prescription. In the picture in which the collisions are viewed as the superposition of independent nucleon-nucleon collisions, one

expects the  $A$  dependence of the  $E_T$  distribution to be given simply through the dependence on  $E^*$ . Thus we introduce the parametrization  $E_T \propto E^* A^\alpha$ , and assert that a nonzero value of  $\alpha$  indicates a departure from this simple picture. We determine  $\alpha$  directly from the present set of data.

The E814/E877 apparatus is described elsewhere [3–5]. A unique feature of the setup is its nearly  $4\pi$  calorimetric coverage: the target calorimeter (TCal) covers the backward hemisphere ( $-0.5 < \eta < 0.8$ ) while the participant calorimeter (PCal) measures energy flow in the forward hemisphere ( $0.83 < \eta < 4.7$ ). The pseudorapidity  $\eta$  is defined as  $\eta = -\ln \tan(\theta/2)$ . PCal is a scintillator tile calorimeter with lead/iron absorber, 4 absorption lengths deep, read out with photomultiplier tubes via optical fibers. It is segmented transversely into 8 radial and 16 azimuthal segments and longitudinally into 4 depth segments, for a total of 512 towers. The resolution is  $45\%/\sqrt{E(\text{GeV})}$  for hadronic showers and  $28\%/\sqrt{E}$  for electromagnetic showers [6]. TCal is made of 992 NaI crystals 5.3 radiation lengths deep. Measurements of the transverse energy production reported here were carried out with PCal and TCal as the principal detectors. The analysis procedures for TCal are described in [3, 4], and the details of PCal construction and calibration are given in [6].

The data are taken with an interaction trigger formed by requiring a PCal analog trigger sum above a modest ( $\sim 1$  GeV) threshold, in coincidence with a valid beam particle. Higher level triggers are formed independently for PCal and TCal based on the  $E_T$  values deposited in either detector. Events are rejected if a second beam particle passes through the beam telescope within  $1 \mu\text{s}$  of the beam particle initiating the trigger.

Corrections for interactions which occur upstream of the target were performed using data taken with an empty target frame. The correction is important (up to 70%) only at low  $E_T$ . For  $dE_T/d\eta$  measurements, the empty target subtraction is made separately for each  $\eta$  bin.

For data from the PCal, transverse energies corrected for leakage and detector response are obtained using a Monte Carlo-generated response matrix. Since the central points made in this Letter crucially depend on knowledge of the  $E_T$  scale, we describe briefly the novel method used here. A complete account of this procedure is given in [7]. The response matrix approach takes into account the known response of the calorimeter to different particles [6] as well as leakage of showers through its sides and back. The calorimeter response is studied using a fast energy deposition program PROPHET, based on the shower parametrization of Bock *et al.* [8]. The program contains the full geometrical detail of PCal and also accounts for missing channels. The detector response matrix  $\mathbf{M}$  is obtained by processing Monte Carlo events through PROPHET and relating the “true”  $E_T$  distribution represented by an 8 element array  $\vec{\alpha}$  of  $E_T$  values, binned in

$\eta$  to match the PCal geometry, to a 32 element “experimental” array  $\vec{D}$ , through the matrix relation  $\mathbf{M}\vec{\alpha} = \vec{D}$ . The elements of  $\vec{D}$  are defined as

$$D_i = \sum_{j=1}^{16} E_{ij} s_{ij} \quad (i = 1, \dots, 32),$$

in which  $j$  is an azimuthal index and  $i$  is an index identifying the radial and longitudinal position of the calorimeter tower. Here  $E_{ij}$  is the measured energy in the tower and  $s_{ij}$  is the sine of the polar angle of its geometrical center. Each element of  $\mathbf{M}$  is thus the fraction of  $E_T$  deposited in a given ring from a certain incident polar angular interval. To obtain values for the 8 parameters  $\alpha_i$  from the measured data  $\vec{D}$  we minimize the function

$$Q^2(\vec{\alpha}) = \sum_{i=1}^{32} \left( \sum_{k=1}^8 M_{ik} \alpha_k - D_i \right)^2.$$

The  $E_T$  spectra are determined by forming the sum  $E_T = \sum \alpha_i$ , where the  $\alpha_i$  are determined independently for each event. Generally, the distributions of  $dE_T/d\eta$  are well characterized by a Gaussian function [1]. Therefore, in determining  $dE_T/d\eta$  distributions from our data we parametrize the array  $\vec{\alpha}$  as a Gaussian with height  $B$ , centroid  $\eta_0$ , and width  $\sigma_\eta$ .

The unfolded transverse energy distributions depend only very weakly on the particular choice of event generator used to compute the response matrix  $\mathbf{M}$ . This is shown in Fig. 1(a) for the system Si+Pb. Similar results have been obtained for the Au+Au system. We find that

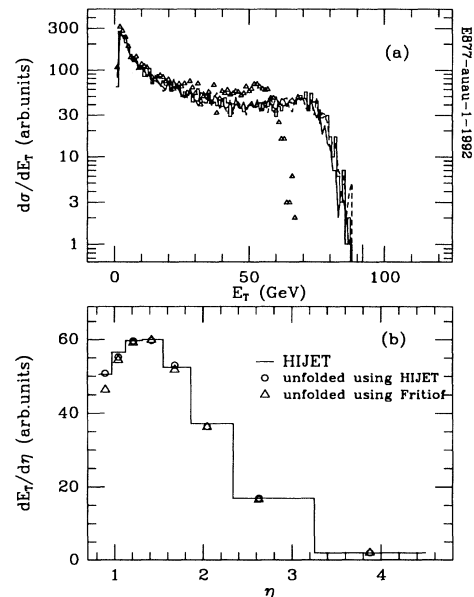


FIG. 1. Test of PCal  $E_T$  correction method. (a) Total  $E_T$  distribution from the event generator HIJET [9] (solid histogram) filtered with the detector response (triangles) and subsequently corrected with the response matrix generated using HIJET (dashed line) or FRITIOF [10] events (solid line). (b) Similar test for the  $dE_T/d\eta$  distribution.

the correction procedure introduces a systematic error in the overall  $E_T$  scale of at most 4%. In Fig. 1(b), a similar study is made for the  $dE_T/d\eta$  distribution. The 7% discrepancy at smallest  $\eta$  between the original results and those found using different response matrices is treated as a systematic error for that value of  $\eta$ . All other systematic uncertainties are estimated to be less than 4%. All PCal data here and below are corrected using the above procedure. As in [3] the TCal  $d\sigma/dE_T$  data are uncorrected.

The distributions  $d\sigma/dE_T$  are compared in Fig. 2 for Au+Au and Si+Al collisions. In both PCal and TCal acceptances a strong increase of  $E_T$  production is observed for the heavier system. The abrupt falloff at large  $E_T$  in the Au+Au distribution shows that fluctuations in the heavier system are significantly reduced as compared to Si+Al collisions (see the short-dashed histogram in Fig. 2). Because of the large difference in shape it is inappropriate to compare  $E_T$  production for the two systems either at a fixed cross section level or for a fixed fraction of the geometrical cross section  $\sigma_{\text{geo}}$ . Rather, following [1], we determine  $E_T^m$ , the mean  $E_T$  for collisions with  $b < 0.5$  fm using different models [9–13] and the fraction  $f = (1/\sigma_{\text{geo}}) \int_{E_T^m}^{\infty} (d\sigma/dE_T) dE_T$ . All models, although predicting significantly different  $E_T$  distributions, yield similar fractions with average values  $f(\text{Si}) = 1.5\%$  and  $f(\text{Au}) = 0.22\%$ . Using the measured data, these fractions determine  $E_T^0$ , the  $E_T$  for an average collision with  $b < 0.5$  fm, as  $E_T^0(\text{Au}) = 318.5$  GeV and  $E_T^0(\text{Si}) = 40.2$  GeV. Thus  $E_T^0$  increases by a factor of 7.9 when going from Si to Au, exceeding the calculated ratio (5.9) of available energies by 34%.

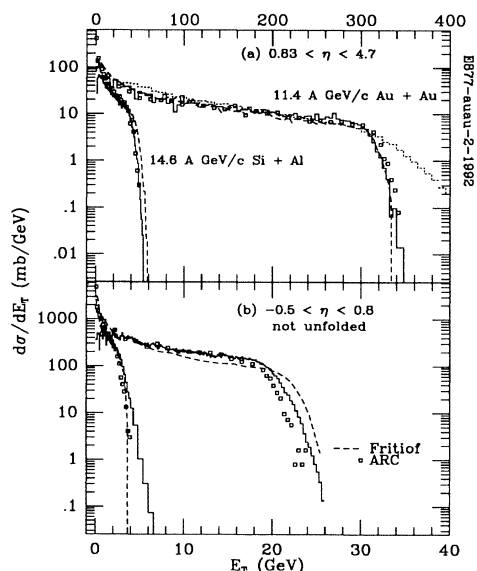


FIG. 2. Data for total  $E_T$  production (histograms) compared with FRITIOF and ARC calculations. Statistical uncertainties are negligible in the data. (a) PCal data. Short-dashed line: Si+Al data scaled up by factor  $E_T^0(\text{Au})/E_T^0(\text{Si})$ . (b) TCal data.

To put our results in context, we have compared the data to predictions from various models. For the comparison with TCal data model calculations are filtered with the detector response using the code GEANT [14]. The comparison to predictions from the hadronic cascade model ARC [13] is shown in Fig. 2, demonstrating good agreement over the full acceptance and for both systems. Results using the Lund string fragmentation model FRITIOF tuned to  $pp$  collisions at AGS energies [10] also reproduce the Au+Au data but overpredict  $E_T^0$  by 14% for the Si+Al system. The RQMD model [12] (not shown), which includes string fragmentation and hadronic cascading, overpredicts the Au+Au data by 14% for the PCal acceptance and underpredicts TCal data by about the same fraction; a similar trend is observed for Si+Al.

Figure 3 shows the measured  $dE_T/d\eta$  distributions of Au+Au and Si+Al events for very central collisions ( $E_T > E_T^0$ ). The corrected PCal results are the Gaussian parametrizations of the  $E_T$  distributions. Folding these with the response matrix  $\mathbf{M}$  gives distributions close to the uncorrected PCal data (see Fig. 3), showing the internal consistency of the procedure. The fluctuations in the uncorrected data are not statistical but reflect the assignment of calorimeter towers to certain  $\eta$  bins. The TCal data ( $\eta < 0.8$ ) in this figure are corrected for response, geometrical acceptance, and leakage by tracking events from HIJET through the detector using GEANT, thereby calculating  $\eta$ -dependent correction factors. Data in this figure were obtained with PCal triggers for both detectors.

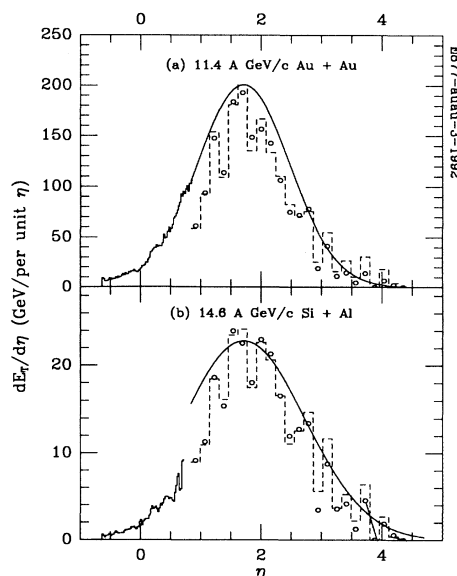


FIG. 3. Corrected  $dE_T/d\eta$  distributions for PCal (Gaussian parametrization, solid curve) and TCal (solid histogram,  $\eta < 0.8$ ) for central collisions ( $E_T > E_T^0$ ). Open circles are the Gaussian curve processed with the response matrix for comparison with the raw data (dashed histograms). For an explanation of their fluctuations see text.

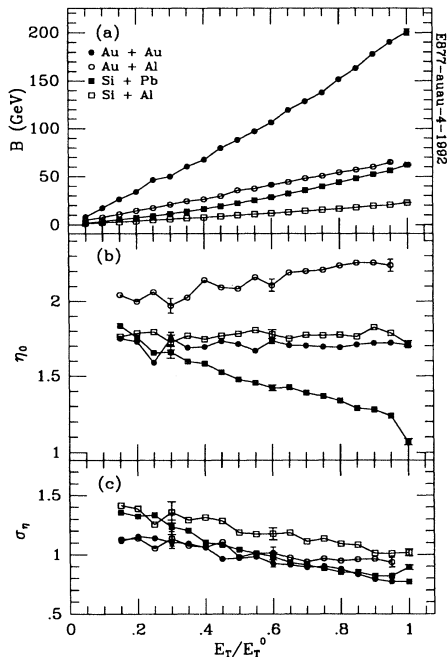


FIG. 4. Parameters of the Gaussian functions representing the PCal ( $0.83 < \eta < 4.7$ )  $dE_T/d\eta$  distributions as a function of  $E_T/E_T^0$ . Typical statistical errors are shown for three centralities.

A comprehensive picture of the evolution of  $E_T$  production in systems of different size is given in Fig. 4, where we present the Gaussian parameters  $B$ ,  $\eta_0$ , and  $\sigma_\eta$  vs  $E_T/E_T^0$  for four different systems: Si+Al, Au+Au, Si+Pb, and Au+Al. The peak value  $B$  of the  $dE_T/d\eta$  distribution continues to grow for all systems as the centrality increases. An interesting feature of the centroid  $\eta_0$  for various systems is displayed in Fig. 4(b). It shows a clear dependence on the symmetry of the system, due to the kinematics of the collision: as the centrality increases, the effective center of mass shifts forward for the Au+Al system; thus the centroid of  $dE_T/d\eta$  moves toward larger  $\eta$ . The opposite dependence can be seen in the Si+Pb system where the centroid moves backward as the centrality of the collision increases. As expected, no shifts are observed for the symmetric systems of Au+Au and Si+Al, where the center of mass does not depend on the centrality. The width parameter  $\sigma_\eta$  decreases for all systems as the centrality increases [Fig. 4(c)]; similar trends have been observed for  $E_T$  [15] and multiplicity [5] distributions measured with light projectiles. This narrowing of the  $E_T$  distribution is directly related to the increase in its height, since the ratio of the products  $B\sigma_\eta \propto \int (dE_T/d\eta)d\eta$  for the two systems is found to be close to the ratio of their  $E_T^0$  values.

These results allow us to determine the scaling parameter  $\alpha$  introduced above to characterize the evolution with mass number of  $E_T$  production. The overall increase in  $E_T^0$  by a factor of 7.9 when going from Si to Au projectiles corresponds to  $\alpha = 0.14 \pm 0.02$ . At midrapidity,  $E_T$

increases even more rapidly, by a factor of 8.8, because of the narrowing of the  $dE_T/d\eta$  distribution for the heavier system (see Fig. 4), yielding a value at midrapidity of  $\alpha = 0.20 \pm 0.02$ . This large value of  $\alpha$  implies a factor of  $(197/27)^{0.2} = 1.49$  increased  $E_T$  production compared to what is expected for independent nucleon-nucleon collisions. Model comparisons show that such an increase can be associated with a large energy and baryon density achieved in the collisions. Using the ARC model, which agrees with our data, the maximum baryon density reached for Au+Au has been evaluated to be 10.5 times the normal density of nuclear matter [13].

We acknowledge the excellent support provided by the BNL AGS and Tandem staffs, especially by Dr. H. Brown and Dr. K. Woodle. Technical support by R. Hutter, D. Makowiecki, and J. Sondericker, and the efforts of the LANL staff, especially that of J. Boissevain, W. Sondheim, and H. van Hecke in the construction and testing of PCal are gratefully acknowledged. We appreciate the critical comments of B. Jacak over the course of this analysis. This work is supported in part by the DOE, the NSF, the NSERC (Canada), and CNPq (Brazil).

- [1] For a recent review of both CERN and AGS data, see J. Stachel and G.R. Young, *Annu. Rev. Nucl. Part. Sci.* **42**, 237 (1992), and references quoted there.
- [2] See, e.g., G. Baym, in *Proceedings of the International Nuclear Physics Conference, Harrogate, 1986*, IOP Conf. Proc. No. 86 (Institute of Physics and Physical Society, London, 1986), p. 309.
- [3] E814 Collaboration, J. Barrette *et al.*, *Phys. Rev. Lett.* **64**, 1219 (1990).
- [4] E814 Collaboration, J. Barrette *et al.*, *Phys. Rev. C* **45**, 819 (1992).
- [5] E814 Collaboration, J. Barrette *et al.*, *Phys. Rev. C* **46**, 312 (1992).
- [6] J. Simon-Gillo *et al.*, *Nucl. Instrum. Methods Phys. Res., Sect. A* **309**, 427 (1991); D. Fox *et al.*, *Nucl. Instrum. Methods Phys. Res., Sect. A* **317**, 474 (1992).
- [7] Z. Zhang, Ph.D. thesis, University of Pittsburgh, 1993 (to be published).
- [8] R.K. Bock *et al.*, *Nucl. Instrum. Methods Phys. Res.* **186**, 533 (1981).
- [9] T. Ludlam, A. Pfoh, and A. Shor, Brookhaven National Laboratory Report No. 51921, 1985 (unpublished).
- [10] B. Andersson, G. Gustafson, and B. Nilsson-Almqvist, *Nucl. Phys.* **B281**, 289 (1987); J. Costales, E802 Internal Report No. E-802-MEM-8, 1988 (unpublished).
- [11] J. Stachel and P. Braun-Munzinger, *Nucl. Phys.* **A498**, 577c (1989).
- [12] H. Sorge, H. Stöcker, and W. Greiner, *Ann. Phys. (N.Y.)* **192**, 266 (1989).
- [13] Y. Pang, T. J. Schlagel, and S. H. Kahana, *Phys. Rev. Lett.* **68**, 2743 (1992); (private communication).
- [14] R. Brun *et al.*, Geant 3.15 User's Guide, CERN Data Handling Division Report No. DD/EE/84-1, revised 92-1, 1992 (unpublished).
- [15] E802 Collaboration, T. Abbott *et al.*, *Phys. Rev. C* **45**, 2933 (1992).